C–H Activation

DOI: 10.1002/anie.201006587

Tuning a P450 Enzyme for Methane Oxidation**

*Felipe E. Zilly, Juan P. Acevedo, Wojciech Augustyniak, Alfred Deege, Ulrich W. Häusig, and Manfred T. Reetz**

Cytochrome P450 (CYP) enzymes are heme-dependent monooxygenases that catalyze the oxidation of C–H bonds of endogenous and exogenous organic compounds with formation of the respective alcohols.[1] The mechanism involves the intermediacy of a high-spin oxyferryl porphyrin radical cation which abstracts a hydrogen atom from the substrate, and the short-lived alkyl radical then undergoes C–O bond formation. The binding pockets of CYPs are relatively large, therefore small compounds do not have a statistically high enough probability of being properly oriented near the oxyferryl moiety for rapid oxidation to occur; additionally there are other effects that slow down or prevent catalysis. A notorious challenge is the oxidation of methane to methanol by chemical catalysis[2] or using enzymes of the type methane monooxygenases (MMOs).[3] It is not only the smallest alkane, but also has the strongest C–H bond (104 kcal mol^{-1}). Although CYPs represent a superfamily of monooxygenases, none have been shown to accept methane, whereas MMOs are complex enzymes (many membrane bound) that have not been expressed in heterologous hosts in any significant quantities, among other problems.[3] Herein we show that chemical tuning of a CYP, which is based on guest/host activation using perfluoro carboxylic acids as chemically inert guests, activates the enzyme for oxidation of not only medium-sized alkanes such as *n*-hexane, but also of small gaseous molecules such as propane and even methane as the ultimate challenge.

In the present study we chose, for practical reasons, the enzyme P450 BM3 (CYP102A1) from *Bacillus megaterium*, which is a self-sufficient fusion protein composed of a P450 monooxygenase and an NADPH diflavin reductase.[4] Several crystal structures of this CYP harboring a fatty acid or fatty acid derived inhibitors, as well in the absence of such compounds have been published.[5] To engineer mutants of P450 BM3 and of other CYPs for enhanced activity and selectivity toward a variety of different compounds, including such difficult substrates as small alkanes, rational design as well as directed evolution have proven to be successful to some extent.[1c,6] For example, P450 BM3 variants characterized by numerous point mutations were obtained in extensive laboratory evolution, and showed for the first time notable activity toward propane by formation of the respective alcohols (2-propanol/1-propanol = 9:1);[6a] however, the ethane to ethanol conversion remains problematic[6b] and methane oxidation has not been achieved to date. Higher activity in ethane oxidation was accomplished using mutants of P450cam,[6c] but here again methane oxidation was not reported. Our chemical approach involves a chemically inert compound that serves as a guest in the binding pocket of P450 BM3, thereby filling the space and reducing the translational freedom of small alkanes or of any other substrate. On the basis of previous reports involving CYPs harboring various substrates,[1] such guest/host interactions can be expected to induce other modes of activation effects as well, specifically water displacement at the Fe/heme site accompanied by a change in the electronic state from the inactive low-spin state to the catalytically active high-spin states.[1,5d] Moreover, many studies have shown that P450 enzymes and mutants thereof can harbor two different substrates simultaneously, thus leading to cooperative effects;[1,7–9] one example is lauric acid and palmitic acid in which cooperativity has been demonstrated by isotope labeling experiments.[8] In yet another study regarding the metabolism of bilirubin, the addition of lauric acid or the perfluorinated analogue was reported to facilitate NADPH oxidation and substrate degradation, a finding that has implications for the treatment of jaundice, uroporphyria, and possibly cancer.[9] It has also been shown for the case of a distantly related H_2O_2-dependent P450 enzyme that its peroxidase activity can be influenced by the addition of fatty acids, wherein increased or decreased activity is observed depending upon their chain length.[10]

In our endeavor we were guided by the binding mode of the natural substrates, fatty acids, of P450 BM3. The binding includes H-bonds originating from their carboxy function and residues Arg 47 and Tyr 51, as well as hydrophobic interactions.[5] The use of perfluoro carboxylic acids such as **1a–h** as chemically inert, yet activating guests was therefore envisioned, because perfluoro alkyl groups are known to be resistant to oxidation while having a hydrophobic character.[11] Moreover, it is known that a CF_3 residue is sterically comparable to a $CH(CH_3)_2$ group,[11a] which means that a perfluoro fatty acid fills much more space in a P450 binding pocket than a traditional fatty acid, and can additionally induce the crucial low-spin to high-spin conversion of Fe/heme.

$CF_3(CF_2)_nCO_2H$

1a: $n = 0$
1b: $n = 5$
1c: $n = 7$
1d: $n = 8$
1e: $n = 9$
1f: $n = 10$
1g: $n = 11$
1h: $n = 12$

In exploratory studies, the oxidation of *n*-octane and *n*-hexane as well as isomers thereof was studied using P450

[*] Dr. F. E. Zilly, Dr. J. P. Acevedo, Dr. W. Augustyniak, A. Deege, U. W. Häusig, Prof. M. T. Reetz
Max-Planck-Institut für Kohlenforschung
Kaiser-Wilhelm-Platz 1, 45470 Mülheim an der Ruhr (Germany)
reetz@mpiso-muelheim.mpg.de

[**] We thank Heike Hinrichs, Frank Kohler, and Sylvia Ruthe for help with the chromatographic measurements.

Supporting information for this article is available on the WWW under http://dx.doi.org/10.1002/anie.201006587.

BM3 as the catalyst in both the absence and presence perfluoro carboxylic acid **1** ($n \geq 7$) under defined reaction conditions. A small amount of dimethylformamide (DMF; 1% v/v) served as the solubilizing cosolvent as part of the standard reaction conditions (Table 1). The results reveal

Table 1: Oxidation of alkanes catalyzed by P450 BM3 in the presence and absence of a perfluoro carboxylic acid **1**.[a]

Alkane	Additive	Total product formed [mM]	TON	Regioselectivity
2	none	0.15	150	2-/3-/4-octanol = 12:44:44
2	**1c**	1.16	1184	2-/3-/4-octanol = 10:42:48
3	none	0.43	149	2-/3-hexanol = 83:17
3	**1e**	1.50	525	2-/3-hexanol = 77:23
4	none	0.36	126	2-hydroxy-3-methyl-/3-hydroxy-3-methylpentane = 89:11
4	**1c**	1.36	476	2-hydroxy-3-methyl-/3-hydroxy-3-methylpentane = 88:12
5	none	0.12	111	only 2-hydroxy-3,3-dimethylbutane
5	**1c**	0.96	891	only 2-hydroxy-3,3-dimethylbutane
6	none	0.02	20	only 2-hydroxy-2,3-dimethylbutane
6	**1e**	0.19	3241	only 2-hydroxy-2,3-dimethylbutane

[a] Reaction conditions: 3.2 mM alkane, 1% v/v DMF, 2% v/v ethanol, 100 mM glucose, 1 mM $NADP^+$, 1 U mL^{-1} GDH, 1 mM additive, 100 mM KPi, pH 8.0, total volume 20 mL, 1 h, 20°C.

some remarkable effects. In all cases the presence of a perfluoro carboxylic acid leads to an increase in the total amount of alcohol product formed, and the turn over number (TON) increases by factors ranging between 4 and 12. In contrast, regioselectivity increases by the presence of an inert guest only to a small extent. Apparently, the presence of perfluoro carboxylic acids in the binding pocket does not lead to a single well-defined orientation of such alkanes, which are relatively small and lack functional groups for additional anchoring. In one case we also focused on stereoselectivity by measuring the enantiomeric excess (% *ee*) of 2-hexanol formed in the oxidation of *n*-hexane (**3**). In the absence of

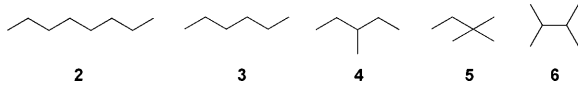

the activator, the *ee* value was found to be 35% in favor of the *R* alcohol, whereas when using **1e** as an activator the enantioselectivity increased to 44% *ee* (*R*). The difference is small, but measurable, indicating that stereoselectivity can in fact be influenced even when reacting such small nonfunctionalized compounds. When subjecting functionalized compounds to P450-BM3-catalyzed hydroxylation in the presence of perfluoro carboxylic acids, notable effects on regio- and stereoselectivity are more likely. When testing iso-hexanes, products arising from the oxidation of methyl groups could not be detected.

We then turned to the smaller gaseous substrates *n*-butane and propane, and this time tested a wider range of perfluoro carboxylic acids **1**. As before, significant increases in product formation and in TON were observed (Table 2), and they depend to some extent on the nature of the perfluoro carboxylic acid. For example, in the case of *n*-butane, the efficiency is highest when using perfluoro carboxylic acid **1b**

Table 2: Oxidation of *n*-butane and propane catalyzed by P450 BM3 in the presence and absence of an additive **1** under standard reaction conditions.[a]

Alkane	Additive	Total product formed [mM]	TON	*ee* [%]
n-butane	none	1.2	527	24
n-butane	**1a**	1.1	469	32
n-butane	**1b**	8.4	3632	22
n-butane	**1c**	2.0	879	23
n-butane	**1d**	3.9	1699	20
n-butane	**1e**	5.8	2519	19
propane	**1e**	3.0	1021	–
propane	**1f**	0.67	227	-
propane	**1h**	0.50	170	–

[a] Reaction conditions: 2.5 mL reaction volume, 5 mL gas volume, 100 mM KPi, pH 8.0, 10 bar pressure (10% butane, 8% O_2, 82% N_2; 7% propane, 8% O_2, 85% N_2), 25°C.

(TON = 3632). Notably, trifluoroacetic acid (**1a**) exerts no activating effect, and the turnover is approximately the same (TON = 469) as in that for the reaction lacking this additive (TON = 527). Products resulting from the oxidation of methyl groups in *n*-butane or propane were not formed (< 1%). In the case of propane, which is essentially not accepted by P450 BM3 in the absence of an activating additive, the most striking effect was observed when using **1e**, which resulted in highest activity (TON = 1021). This is still lower than the reported activity of a P450 BM3 mutant obtained by directed evolution,[6a] but our approach is simple to perform and does not require protein engineering. Moreover, unlike the results of the protein engineering study,[6a] we observe complete regioselectivity in favor of 2-propanol.

In ultimate experiments, we considered the oxidation of methane, which is also not accepted by P450 BM3. To obtain reliable data regarding small amounts of methanol formation in an aqueous medium, the sensitive LaCourse method of pulsed amperometric detection of aliphatic alcohols was used[12] and coupled with GC/MS measurements (see the Supporting Information). Gratifyingly, high turnover numbers were observed as a consequence of adding the appropriate perfluoro carboxylic acids (Table 3). As before, the activity depends upon the chain length of the perfluoro fatty acid and achieves a maximum of TON = 2472 in the case of **1d**. Presently it is difficult to interpret the observed "trend", inter alia because perfluoro fatty acids are sterically quite different from their nonfluorinated counterparts.

In an effort to unveil the origin of enhanced activity induced by the appropriate perfluoro carboxylic acids **1**, biophysical and computational investigations were carried out. It was particularly important to obtain evidence showing that the perfluoro carboxylic acids do in fact exert their activating effects as chemically inert guests in the binding

Table 3: Oxidation of methane into methanol catalyzed by P450 BM3 in the presence of an additive **1** under standard reaction conditions.[a]

Additive	Total product formed [mM]	TON
1c	2.75	2053
1d	3.31	2472
1e	1.81	1353
1f	1.25	933
1g	0.75	560
1h	0.28	210

[a] Reaction conditions: 2.5 mL reaction volume, 5 mL gas volume, 100 mM KPi, pH 8.0, 10 bar pressure (7% methane, 8% O_2, 85% N_2), 25 °C.

pocket of P450 BM3. It is known that long-chain substrates, once in the binding pocket of P450 BM3 (and of other CYPs), lead to the displacement of water at the Fe/heme which causes a shift from the low-spin resting state to the catalytically active high-spin state of the metalloenzyme, as indicated by UV/Vis and UV/Vis difference spectra.[1,5d,7] In contrast, most inhibitors either stabilize the water or directly ligate to the Fe/heme, thus favoring the inactive low-spin state. We therefore applied this technique to P450 BM3 in the absence and presence of perfluoroundecanoic acid (**1e**), and for comparison we included the analogous C_{11} fatty acid (undecanoic acid). The anticipated effect was indeed observed, with undecanoic acid and the perfluoro analogue **1e** leading to similar UV/Vis difference spectra (see the Supporting Information). In both cases the spectra show an absorption decrease at 420 nm (low-spin complex) and concomitant increase at 390 nm (high-spin species). This behavior is typical of activated, substrate-bound P450 BM3. In additional experiments, the titration curves resulting from using **1e** (0.1 mM to 16 mM) and P450 BM3, and competition experiments involving *n*-octylamine as an inhibitor (which is known to exert its effect by entering the binding pocket of CYPs[13]) support this conclusion (see the Supporting Information).

We surmise at this stage that two phenomena are likely to be responsible for the guest/host activating effect of perfluoro carboxylic acids. The occurrence of such compounds in the binding pocket not only reduces its effective volume, but it also leads to partial conversion of the low-spin species into a catalytically active high-spin Fe species, probably induced by the displacement of water at the Fe/heme.[1,5d,7] In line with this proposition is the observation that trifluoroacetic acid (**1a**) fails to show any activating effect.

To gain additional insight, we turned to molecular dynamics (MD) simulations.[14] Following MD calculations of P450 BM3 in the absence of any ligand, the Gromos algorithm was applied,[15] leading to the visualization of an ensemble of different conformers. Subsequently, perfluorodecanoic acid (**1d**), which caused the highest activity in methane oxidation (Table 3), was successfully docked in the average minimized structure of the most populated cluster of P450 BM3 conformers. A second MD calculation was then performed of the enzyme harboring the activator **1d** and simulating the experimental conditions of methane concentration and pressure (see the Supporting Information). It was found that **1d** adopts two different binding modes of essentially equal energy. In binding mode I the carboxy function interacts with Tyr51 and Ser72 through hydrogen bonds that allow the end of the perfluoro chain to lie very deeply in the binding pocket near the Fe/heme, thereby distinctly reducing space. Binding mode II is characterized by hydrogen bonds between the carboxy function and Arg47, which in this case prevents such deep penetration of the perfluoro chain. Space around and near the active Fe site is therefore considerably larger. The simulations do not provide accurate information as to whether the water at Fe/heme is displaced by activator **1d** as actually indicated by the UV/Vis difference spectra.

In the final step of the computational analysis, docking experiments using methane in the presence and absence of activator **1d** were performed (see the Supporting Information), and they led to some remarkable results. In the case of **1d** undergoing binding mode I with a reduced space around the active site, a cluster of methane molecules lies directly above Fe/heme, perfectly juxtaposed for rapid oxidation (Figure 1). In the case of binding mode II, methane distributes throughout the distinctly larger cavity, presumably leading to lower or no activity. In neither of the cases above nor in the absence of an activating guest was any reorientation of the phenyl group of Phe87 with concomitant shielding of the oxyferryl porphyrin radical cation observed; this shielding would slow down catalysis as reported for certain other substrates.[1,4–7]

In the absence of the activator **1d**, the binding pocket is dramatically larger, and the Glide algorithm[15] does not predict any specific positioning of methane clusters (see the

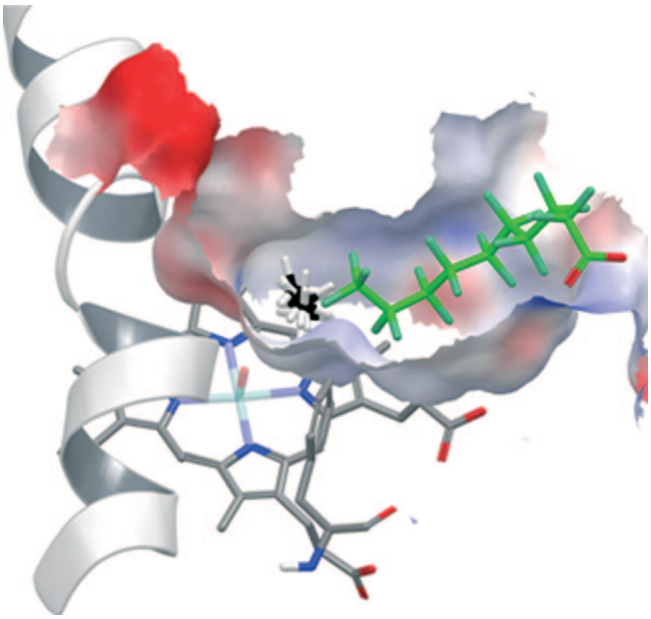

Figure 1. Binding pocket representation of P450 BM3 harboring activator **1d** (perfluoro chain in green) and docking poses of a methane cluster (carbon atoms in black and hydrogen atoms in white) hovering above Fe=O (red) in the porphyrin ring. Binding pocket surface is colored according to its electrostatic potential (red: positive, blue: negative, white: neutral). Helix I is shown as a point of reference.

Supporting Information). It remains to be seen whether such extensive computational analyses of the other perfluoro carboxylic acids used in the present study will reflect the observed dependency on chain length (Table 3).

In conclusion, we have implemented a chemical strategy for tuning the catalytic profile of the monooxygenase P450 BM3 so that the enzyme accepts such notoriously difficult substrates as propane and methane and results in the formation of the respective alcohols. We expect ethane[6b,c] to behave similarly. In contrast to time-consuming protein engineering,[6] the present approach simply requires the addition of an appropriate chemically inert perfluoro fatty acid to the enzyme, thereby triggering a catalytically activating effect which originates from specific guest/host interactions in the binding pocket. A shift from an inactive low-spin state to a catalytically active high-spin state and a decrease in the effective volume of the binding pocket appear to be the crucial factors as shown by UV/Vis difference spectra as well as a theoretical analysis based on MD simulations and docking experiments. The present approach not only allows methane to be oxidized with notable enzyme activity, but also opens the door for using perfluoro carboxylic acids, which can be expected to bind to most CPYs, to influence the catalytic profile of monooxygenases as catalysts in the functionalization of more complex organic compounds, including the control of regio- and stereoselectivity.[16] The size of the perfluoro carboxylic acid can then be matched to the specific requirements, which depend upon the steric and electronic nature of the to-be-oxidized substrate, with MD simulations serving as a guide. The use of chiral perfluoro carboxylic acids or of other types of chemically inert perfluoro compounds as additives for influencing stereoselective oxidative hydroxylation is yet another perspective. Finally, we anticipate that the combination of the present tuning method with protein engineering techniques[6] constitutes a powerful tool for controlling regio- and stereoselective P450-catalyzed C–H activation.

Received: October 20, 2010
Revised: January 1, 2011
Published online: February 17, 2011

Keywords: alkanes · C–H activation · host–guest systems · methane oxidation · P450 enzymes

[1] a) P. R. Ortiz de Montellano, *Cytochrome P450: Structure, Mechanism, and Biochemistry*, 3rd ed., Springer, Berlin, **2005**; b) E. M. Isin, F. P. Guengerich, *Biochim. Biophys. Acta Gen. Subj.* **2007**, *1770*, 314–329; c) A. W. Munro, H. M. Girvan, K. J. McLean, *Nat. Prod. Rep.* **2007**, *24*, 585–609; d) I. G. Denisov, T. M. Makris, S. G. Sligar, I. Schlichting, *Chem. Rev.* **2005**, *105*, 2253–2277; e) V. Cojocaru, P. J. Winn, R. C. Wade, *Biochim. Biophys. Acta Gen. Subj.* **2007**, *1770*, 390–401; f) S. Shaik, S. Cohen, Y. Wang, H. Chen, D. Kumar, W. Thiel, *Chem. Rev.* **2010**, *110*, 949–1017; g) T. Furuya, K. Kino, *Appl. Microbiol. Biotechnol.* **2010**, *86*, 991–1002; h) J. T. Groves, *J. Inorg. Biochem.* **2006**, *100*, 434–447; i) S. Shaik, S. P. de Visser, F. Ogliaro, H. Schwarz, D. Schröder, *Curr. Opin. Chem. Biol.* **2002**, *6*, 556–567; j) R. D. Bach, *J. Phys. Chem. A* **2010**, *114*, 9319–9332; k) D. Kumar, B. Karamzadeh, G. N. Sastry, S. P. de Visser, *J. Am. Chem. Soc.* **2010**, *132*, 7656–7667.

[2] Methane oxidation by chemical catalysts or reagents: a) J. A. Labinger, J. E. Bercaw, *Nature* **2002**, *417*, 507–414; b) I. Hermans, E. S. Spier, U. Neuenschwander, N. Turrà, A. Baiker, *Top. Catal.* **2009**, *52*, 1162–1174; c) H. Arakawa, M. Aresta, J. N. Armor, M. A. Barteau, E. J. Beckman, A. T. Bell, J. E. Bercaw, C. Creutz, E. Dinjus, D. A. Dixon, K. Domen, D. L. DuBois, J. Eckert, E. Fujita, D. H. Gibson, W. A. Goddard, D. W. Goodman, J. Keller, G. J. Kubas, H. H. Kung, J. E. Lyons, L. E. Manzer, T. J. Marks, K. Morokuma, K. M. Nicholas, R. Periana, L. Que, J. Rostrup-Nielson, W. M. H. Sachtler, L. D. Schmidt, A. Sen, G. A. Somorjai, P. C. Stair, B. R. Stults, W. Tumas, *Chem. Rev.* **2001**, *101*, 953–996; d) G. A. Olah, A. Goeppert, G. K. S. Prakash, *Beyond Oil and Gas: The Methanol Economy*, Wiley-VCH, Weinheim, **2006**; e) B. L. Conley, W. J. Tenn III, K. J. H. Young, S. K. Ganesh, S. K. Meier, V. R. Ziatdinov, O. Mironov, J. Oxgaard, J. Gonzales, W. A. Goddard III, R. A. Periana, *J. Mol. Catal. A* **2006**, *251*, 8–23; f) N. Dietl, M. Engeser, H. Schwarz, *Angew. Chem.* **2009**, *121*, 4955–4957; *Angew. Chem. Int. Ed.* **2009**, *48*, 4861–4863; g) D. Schröder, *Angew. Chem.* **2010**, *122*, 862–863; *Angew. Chem. Int. Ed.* **2010**, *49*, 850–851.

[3] Methane oxidation by methane monooxygenases: a) M. Merkx, D. A. Kopp, M. H. Sazinsky, J. L. Blazyk, J. Müller, S. J. Lippard, *Angew. Chem.* **2001**, *113*, 2860–2888; *Angew. Chem. Int. Ed.* **2001**, *40*, 2782–2807; b) R. A. Himes, K. Barnese, K. D. Karlin, *Angew. Chem.* **2010**, *122*, 6864–6866; *Angew. Chem. Int. Ed.* **2010**, *49*, 6714–6716; c) C. E. Tinberg, S. J. Lippard, *Biochemistry* **2010**, *49*, 7902–7912; d) R. Balasubramanian, S. M. E. Smith, S. Rawat, L. A. Yatsunyk, T. L. Stemmler, A. C. Rosenzweig, *Nature* **2010**, *465*, 115–119; e) D. J. Leak, R. A. Sheldon, J. M. Woodley, P. Adlercreutz, *Biocatal. Biotransform.* **2009**, *27*, 1–26; f) D. E. Torres Pazmino, M. Winkler, A. Glieder, M. W. Fraaije, *J. Biotechnol.* **2010**, *146*, 9–24; g) R. K. Thauer, *Angew. Chem.* **2010**, *122*, 6862–6863; *Angew. Chem. Int. Ed.* **2010**, *49*, 6712–6713.

[4] a) L. O. Narhi, A. J. Fulco, *J. Biol. Chem.* **1986**, *261*, 7160–7169; b) A. W. Munro, D. G. Leys, K. J. McLean, K. R. Marshall, T. W. B. Ost, S. Daff, C. S. Miles, S. K. Chapman, D. A. Lysek, C. C. Moser, C. C. Page, P. L. Dutton, *Trends Biochem. Sci.* **2002**, *27*, 250–257; c) T. Jovanovic, R. Farid, R. A. Friesner, A. E. McDermott, *J. Am. Chem. Soc.* **2005**, *127*, 13548–13552; d) K. H. Clodfelter, D. J. Waxman, S. Vajda, *Biochemistry* **2006**, *45*, 9393–9407.

[5] a) K. G. Ravichandran, S. S. Boddupalli, C. A. Hasermann, J. A. Peterson, J. Deisenhofer, *Science* **1993**, *261*, 731–736; b) H. Li, T. L. Poulos, *Nat. Struct. Biol.* **1997**, *4*, 140–146; c) I. F. Sevrioukova, H. Li, H. Zhang, J. A. Peterson, T. L. Poulos, *Proc. Natl. Acad. Sci. USA* **1999**, *96*, 1863–1868; d) D. C. Haines, D. R. Tomchick, M. Machius, J. A. Peterson, *Biochemistry* **2001**, *40*, 13456–13465; e) D. C. Haines, B. Chen, D. R. Tomchick, M. Bondlela, A. Hegde, M. Machius, J. A. Peterson, *Biochemistry* **2008**, *47*, 3662–3670.

[6] Examples of protein engineering studies of P450 enzymes: a) R. Fasan, M. M. Chen, N. C. Crook, F. H. Arnold, *Angew. Chem.* **2007**, *119*, 8566–8570; *Angew. Chem. Int. Ed.* **2007**, *46*, 8414–8418; b) P. Meinhold, M. W. Peters, M. M. Y. Chen, K. Takahashi, F. H. Arnold, *ChemBioChem* **2005**, *6*, 1765–1768; c) F. Xu, S. G. Bell, J. Lednik, A. Insley, Z. Rao, L.-L. Wong, *Angew. Chem.* **2005**, *117*, 4097–4100; *Angew. Chem. Int. Ed.* **2005**, *44*, 4029–4032; d) S. Brenner, S. Hay, H. M. Girvan, A. W. Munro, N. S. Scrutton, *J. Phys. Chem. B* **2007**, *111*, 7879–7886; e) A. Glieder, E. T. Farinas, F. H. Arnold, *Nat. Biotechnol.* **2002**, *20*, 1135–1139; f) D. Appel, S. Lutz-Wahl, P. Fischer, U. Schwaneberg, R. D. Schmid, *J. Biotechnol.* **2001**, *88*, 167–171; g) V. B. Urlacher, S. Eiben, *Trends Biotechnol.* **2006**, *24*, 324–330; h) M. W. Peters, P. Meinhold, A. Glieder, F. H. Arnold, *J. Am.*

Chem. Soc. **2003**, *125*, 13442 – 13450; i) S. Kumar, J. R. Halpert, *Biochem. Biophys. Res. Commun.* **2005**, *338*, 456 – 464; j) C.-K. J. Chen, R. E. Berry, T. K. Shokhirveva, M. B. Murataliev, H. Zhang, F. A. Walker, *J. Biol. Inorg. Chem.* **2010**, *15*, 159 – 174; k) J. D. Ryan, R. H. Fish, D. S. Clark, *ChemBioChem* **2008**, *9*, 2579 – 2582; l) Y. Fujii, H. Kabumoto, K. Nishimura, T. Fujii, S. Yanai, K. Takeda, N. Tamura, A. Arisawa, T. Tamura, *Biochem. Biophys. Res. Commun.* **2009**, *385*, 170 – 175; m) T. Uno, E. Mitchell, K. Aida, M. H. Lambert, T. A. Darden, L. G. Pedersen, M. Negishi, *Biochemistry* **1997**, *36*, 3193 – 3198; n) H. Kabumoto, K. Miyazaki, A. Arisawa, *Biosci. Biotechnol. Biochem.* **2009**, *73*, 1922 – 1927; o) S. Kumar, *Expert Opin. Drug Metab. Toxicol.* **2010**, *6*, 115 – 131; p) R. Bernhardt, *J. Biotechnol.* **2006**, *124*, 128 – 145; q) I. Axarli, A. Prigipaki, N. E. Labrou, *Biomol. Eng.* **2005**, *22*, 81 – 88; r) A. M. Sawayama, M. M. Y. Chen, P. Kulanthaivel, M.-S. Kuo, H. Hemmerle, F. H. Arnold, *Chem. Eur. J.* **2009**, *15*, 11723 – 11729; s) R. J. F. Branco, A. Seifert, M. Budde, V. B. Urlacher, M. J. Ramos. J. Pleiss, *Proteins Struct. Funct. Genet.* **2008**, *73*, 597 – 607; t) J. A. Dietrich, Y. Yoshikuni, K. J. Fisher, F. X. Woolard, D. Ockey, D. J. McPhee, N. S. Renninger, M. C. Y. Chang, D. Baker, J. D. Keasling, *ACS Chem. Biol.* **2009**, *4*, 261 – 267.

[7] a) M. A. Noble, K. L. Turner, S. K. Chapman, A. W. Munro, *Biochem. Soc. Trans.* **1998**, *26*, S213; b) Y.-F. Ueng, T. T. Kuwabara, Y.-J. Chun, F. P. Guengeric, *Biochemistry* **1997**, *36*, 370 – 381; c) K. R. Korzekwa, N. Krishnamachary, M. Shou, A. Ogai, R. A. Parise, A. E. Rettie, F. J. Gonzales, T. S. Tracy, *Biochemistry* **1998**, *37*, 4137 – 4147; d) B. J. Baas, I. G. Denisov, S. G. Sligar, *Arch. Biochem. Biophys.* **2004**, *430*, 218 – 228; e) W. M. Atkins, *Annu. Rev. Pharmacol. Toxicol.* **2005**, *45*, 291 – 310; f) H. Fernando, J. R. Halpert, D. R. Davydov, *Biochemistry* **2006**, *45*, 4199 – 4209; g) K. A. Feenstra, E. B. Starikov, V. B. Urlacher, J. N. M. Commandeur, N. P. E. Vermeulen, *Protein Sci.* **2007**, *16*, 420 – 431; h) Y. Kapelyukh, M. J. I. Paine, J.-D. Marechal, M. J. Sutcliffe, C. R. Wolf, G. C. K. Roberts, *Drug Metab. Dispos.* **2008**, *36*, 2136 – 2144; i) M. Shou, Y. Lin, P. Lu, C. Tang, Q. Mei, D. Cui, W. Tang, J. S. Ngui, C. C. Lin, R. Singh, B. K. Wong, J. A. Yergey, J. H. Lin, P. G. Pearson, T. A. Baillie, A. D. Rodrigues, T. H. Rushmore, *Curr. Drug Metab.* **2000**, *2*, 17 – 36; j) See also discussions in citations.[5]

[8] D. A. Rock, B. N. S. Perkins, J. Wahlstrom, J. P. Jones, *Arch. Biochem. Biophys.* **2003**, *416*, 9 – 16.

[9] N. Pons, S. Pipino, F. De Matteis, *Biochem. Pharmacol.* **2003**, *66*, 405 – 414.

[10] a) O. Shoji, T. Fujishiro, H. Nakajima, M. Kim, S. Nagano, Y. Shiro, Y. Watanabe, *Angew. Chem.* **2007**, *119*, 3730 – 3733; *Angew. Chem. Int. Ed.* **2007**, *46*, 3656 – 3659; b) K. S. Rabe, M. Erkelenz, K. Kiko, C. M. Niemeyer, *Biotechnol. J.* **2010**, *5*, 891 – 899.

[11] a) D. M. Lemal, *J. Org. Chem.* **2004**, *69*, 1 – 11; b) B. W. Purse, J. Rebeck, Jr., *Chem. Commun.* **2005**, 722 – 724.

[12] W. R. LaCourse, D. C. Johnson, M. A. Rey, R. W. Slingsby, *Anal. Chem.* **1991**, *63*, 134 – 139.

[13] M. Shebley, U. M. Kent, D. P. Ballou, P. F. Hollenberg, *Drug Metab. Dispos.* **2009**, *37*, 745 – 752.

[14] Schrödinger, LLC Maestro 8.5 User Manual, Schrödinger Press, New York, **2008**.

[15] X. Daura, K. Gademann, B. Jaun, D. Seebach, W. F. van Gunsteren, A. E. Mark, *Angew. Chem.* **1999**, *111*, 249 – 253; *Angew. Chem. Int. Ed.* **1999**, *38*, 236 – 240.

[16] M. T. Reetz, F. E. Zilly, DE 102010045662.4, **2010**.

Angewandte Chemie
Eine Zeitschrift der Gesellschaft Deutscher Chemiker

Supporting Information

69451 Weinheim, Germany

Tuning a P450 Enzyme for Methane Oxidation**

*Felipe E. Zilly, Juan P. Acevedo, Wojciech Augustyniak, Alfred Deege, Ulrich W. Häusig, and Manfred T. Reetz**

anie_201006587_sm_miscellaneous_information.pdf

Experimental Section

Chemical compounds

In general, chemical compounds were purchased from Aldrich. Perfluoro carboxylic acids were purchased from the following sources: **1b** (Aldrich), **1c** (ABCR), **1d** (Aldrich), **1e** (ABCR), **1f** (Acros), **1g** (Aldrich), **1h** (Aldrich), and **1a** (Aldrich).

Plasmid

The gene *p450-bm3/cyp102a1* encoding P450-BM3 from *Bacillus megaterium* (ATTC 14581, DSM32) was cloned into the pETM11 vector (EMBL, Germany) carrying an *N*-terminal polyhistidine tag, as described previously to give the vector pETM11-P450-BM3-WT[1].

Protein expression and purification

E. coli BL21 (DE3) GOLD (Novagen) were transformed with the vector pETM11-P450-BM3-WT. An aliquot of an overnight culture in LB medium, supplemented with kanamycin (20 mg/l) and tetracycline (12.5 mg/l) for selection, was used to inoculate TB medium supplemented with 50 mg/l kanamycin, 0.1 g/l glutamate, 0.4% (v/v) glycerol, trace metals (50 µM $FeCl_3$, 20 µM $CaCl_2$, 10 µM $MnCl_2$, 10 µM $ZnSO_4$, 2 µM $CoCl_2$, 2 µM $CuCl_2$, 2 µM $NiCl_2$, 2 µM Na_2MoO_4, 2 µM H_3BO_3) and 1 mM $MgCl_2$. After cultivation at 37 °C with horizontal shaking at 250 rpm and reaching an OD_{600} of ~ 0.6–0.8, IPTG was added to a final concentration of 100 µM, the temperature reduced to 25 °C and the shaking rate reduced from 250 rpm to 130 rpm. The expression was performed for 24 h. Afterwards, the bacteria were harvested by centrifugation. The pellet was stored at -80 °C until further processing. For lysis of the bacterial cells, the pellet was thawed by adding 50 mL of lysis buffer (25 mM Tris, 20% glycerol, 0.1% Tween-20 and 20 mg/l DNAse I (Applichem, Germany)) per 1 l of initial culture and resuspended. The cells were broken by passing the suspension through a French-press (American Instruments Company, Silverspring, USA) at a pressure of 1200 psi. The collected lysate was centrifuged for 1 h at 18,000 g at 4 °C. Subsequently, the supernatant was further passed through a 0.22 µm filter.

The lysate was desalted using 100 mM Tris/HCl pH 7.8 buffer using HiTrap Desalting 5 mL (GE Healthcare) columns. This and the following chromatography steps were performed using ÄKTA Purifier (GE Healthcare). Protein fractions were collected and subjected to anion exchange[2] chromatography

using Tosoh DEAE-5PW resin (Tosoh Bioscience, Japan) as stationary phase equilibrated using 100 mM Tris-HCl pH 7.8 buffer. The protein was eluted using jump gradient of equilibration buffer containing 1 M NaCl. For spectral analysis, the red colored, enzyme containing fractions were further subjected to gel filtration using Sephacryl S-100 HR (GE Healthcare) and 100 mM Tris-HCl pH 8.0, 150 mM NaCl as elution buffer. Protein fractions were collected, and the enzyme concentration determined by CO difference spectrum analysis[3]. Overall, approximately 0.8 µmol of semi-purified wt P450 BM3 was obtained from 1 l of culture.

Hydroxylation of C_6 and C_8 alkanes:

In order to hydroxylate alkane compounds (C_6 and C_8), the substrate was given from a 160 mM stock in EtOH to a reaction solution with a final concentration of 3.2 mM. The solution further contained 0.1 M glucose (Riedel de Haen), 1 mM $NADP^+$ (Codexis, Jülich, Germany), 1U/ml GDH (#001, Codexis, Jülich, Germany), 1 mM additive (if not specified otherwise), BM3-WT enzyme (for the conversion of compound **2**: 1µM, **3**: 2.9 µM, **4**: 2.9 µM, **5**: 1.1 µM, **6**: 2.7 µM in the final mixture) and 100 mM KPi pH 7.8 to a total volume of 20 ml. The reactions were run over 1 hr at 20 °C in a 50 ml falcon tube shaken in a bacterial incubator set to 130 rpm. After 1 h three aliquots of 1 ml volume each were taken, acidified with 0.1 ml 10% hydrochloric acid. 1 mM 1-pentanol was used as internal reference. The mixture was extracted using half a volume of MTBE and subjected to GC analysis.

Hydroxylation of C_1, C_3 and C_4 alkanes:

Hydroxylation of gaseous alkanes was performed in a self-build low-pressure reactor. Twelve reaction tubes with a total volume of about 7 ml were filled with 2.5 ml reaction mix containing 0.1 M D-glucose (Riedel de Haen), 1 mM $NADP^+$ (Codexis), 1 U/ml GDH (Codexis), 1 mM additive, BM3-WT enzyme (for the conversion of *n*-butane: 2.3 µM, propane: 2.9 µM, methane: 1.3 µM in the final mixture) and 100 mM KPi, pH 8.0. Afterwards, the reaction tubes were connected to a gas bottle via a multi-channel gas supply. The following gas mixtures were used to flush the equipment and to apply a pressure of 10 bar to the reaction mix: a) 7% methane, 8% oxygen, 85% nitrogen; b) 7% propane, 8% oxygen, 85% nitrogen; or c) 10% butane, 8% oxygen, 82% nitrogen, all leading to a reaction mixture comprising approximately 1 mM alkane. The reaction mixture was stirred at 100 rpm using a magnetic stirring bar with a crosshead (VWR) for a) 21,0 , b) 14,5 or c) 17,5 hrs. For termination of the reaction, the pressure

was slowly released from the reaction tubes and an aliquot of 1 ml was centrifuged for 10 min at 13,000 rpm and subjected to HPLC analysis afterwards. Another aliquot of 1 ml was mixed with 0.1 ml 10% hydrochloric acid for later GC analysis. Each experiment contained at least one positive control for enzyme activity, wherein dodecanoic acid was used as additive (1 mM final concentration, added from stock of 100 mM in DMSO) while subjecting the enzyme to 10 bar gaseous alkane-mix. The conversion of dodecanoic acid was analyzed using decanoic acid (1 mM final concentration, added from stock of 100 mM in DMSO) as reference standard. Samples for GC analysis were extracted using 0.5 volumes of MTBE and subjected to GC analysis.

GC analyses

Fatty acids were analyzed by GC using the following setup: 6890N (Agilent, USA); column: 15m DB-Free Fatty Acid Phase, inner diameter of 0.25 mm, film thickness of 0.25 µm, J & W, Germany; pressure: 0.5 bar H2; injector: 220 °C; temperature gradient: 80–240 °C with 8 °C/min, 15 min isothermal. The conversion of lauric acid was calculated by comparison of the peak areas from lauric acid with the reaction standard decanoic acid, taking the fact of a 1.22 times bigger signal area for lauric acid than decanoic acid at the same concentration into account. The product distribution was calculated by setting the product peak areas directly into relation to each other.

Hydroxylation products of *n*-octane, 2,2-dimethyl butane, *n*-hexane, 3-methyl pentane, 2,3-dimethyl butane were analyzed by GC using the following setup: HP6890 + 7683HP (Hewlett Packard, USA); column: 15m Stabilwax Phase, inner diameter of 0.25 mm, film thickness of 0.5 µm, (J&W, Germany); pressure: 0.8 bar H2; split-rate 60; injector: 220 °C; temperature gradient: 40 °C 4 min isothermal, 40–60 °C with 4 °C/min, 60–250 °C with 15 °C/min, FID detector. For quantification, the product peaks were set into relation to the 1 mM 1-pentanol reaction standard peak with the following pre-determined correction factors: 2-octanol: 2.36; 3- and 4-octanol: 2.23; 2- and 3-hexanol: 1.218; 3-methyl-3-pentanol and 3-methyl-2-pentanol: 1.49; 3.3-dimethyl-2-butanol: 1.43; 2,3-dimethylbutanol: 1.317.

Butanol was analyzed by GC using the following setup: HP6890plus + 7683HP (HewletPackard, USA); column: 15m Stabilwax Phase, inner diameter of 0.25 mm, film thickness of 0.5 µm, (J&W, Germany); pressure: 0.8 bar H2; split-rate 60; injector: 220 °C; temperature gradient: 40 °C 4 min isothermal, 40–60 °C with 4 °C/min, 60–250 °C with 15 min, FID detector.

Propanol was analyzed by GC using the following setup: HP6890plus + 7683HP;530 (Hewlett Packard, USA); column: 15m Free Fatty Acid Phase (FFAP) G/366; pressure: 0.5 bar H2; sample size 1 µl; injector: 220 °C; temperature gradient: 80–240 °C with 8 °C/min, 250 °C with 15 min isothermal, FID detector.

Determination of enantiomeric excess (*ee*)

For chiral 2- and 3-hexanol analysis the following setup was employed: AT 6890N (HP Agilent, USA); column: 15m BGB-177/BGB-15 Phase, inner diameter of 0.25 mm, film thickness of 0.25 µm, (BGB Analytik AG, Germany); pressure: 0.5 bar H_2; split-rate 25; injector: 220 °C; temperature gradient: 40–200 °C with 0,5 °C/min, FID detector.

GC-MS analyses

For GC-MS analysis butanol was analyzed using the following setup: SSQ 7000 GC/MS System (Thermo Finnigan, USA); column: 15m DB-Wax Phase, inner diameter of 0.25 mm, film thickness of 0.5 µm, (J&W, Germany); pressure: 0.5 bar He; split-rate 50; injector: 220 °C; temperature gradient: 30–60 °C with 4 °C/min, 60–250 °C with 20 °C/min.

For GC-MS detection of propanol the following setup was employed: GC:HP6890 + MS: HP5973 (HewletPackard, USA); column: 15m DB-Waxetr Phase, inner diameter of 0.25 mm, film thickness of 0.25 µm, J&W, Germany; pressure: 0.5 bar He; split-rate 10; injector: 220 °C; temperature gradient: 40 °C 10 min, 40–240 °C with 16 °C/min.

For GC-MS detection of Methanol the following setup was employed: GC: HP6890 + MS: 5973 (Hewlett Packard, USA); column: 60m Stabilwax Phase, inner diameter of 0.25 mm, film thickness of 0.5 µm (Restek, Germany); pressure: 1.4 bar He; split-rate 5; injector: 220 °C; temperature gradient: 60 °C 30 min isothermal, 60–240 °C with 16 °C/min, 240 °C with 5 min isothermal.

HPLC analyses

HPLC analyses were performed using a LC-10A System, controlled by the LC-Solution Software (Shimadzu Deutschland GmbH, Duisburg, Germany). The modular LC-System was equipped with LC-10AD pumps, a SIL-10A autoinjector, a CTO-10AC Column oven, a differential-refractive-index-

detector RID-10A (all from Shimadzu Deutschland GmbH, Duisburg, Germany) or an electrochemical detector ED 50 (Dionex GmbH, Idstein, Germany).

Separations were carried out with Organic Acid Resin columns (300 mm length, 8 mm i.d. and precolumn 40 mm length, 8 mm i.d; CS-Chromatographie Service GmbH, Langerwehe, Germany) and 10 mM trifluoroacetic acid in water. The separations were performed at 333 K with an eluent flow-rate of 1.0 ml/min.

Determination of 2-propanol, 2-butanol and methanol

In order to determine the formation of the oxidation products of the gaseous alkanes *n*-butane, propane and methane quantitatively in the aqueous medium, refractive index detection (RID) and the LaCourse method of pulsed amperometric detection (PAD) of aliphatic alcohols were employed.[5] This electrochemical detection method is sensitive to even small amounts of alcohols including methanol (see also Application Note 188 of Dionex Corporation). PAD adjustments were made according to instructions of the Dionex Application Laboratory. Quantification of 2-propanol and 2-butanol was performed using the RID-10A detector. In the case of methanol, the ED 50 detector was employed in an integrated amperometric measurement mode using a Ag reference electrode in the range of 300 nC. The measurements were performed in a waveform as follows:

Step	Time (sec)	Potential (V)	
0	0.0	+ 0.4	
1	0.28	+ 0.4	Begin
2	0.30	+ 0.4	End
3	0.31	+ 0.4	
4	0.32	+ 1.4	
5	0.44	+ 1.4	
6	0.45	- 0.4	
7	0.88	- 0.4	

Parallel to this assay, GC/MS analyses was performed to further substantiate the presence of methanol:

First, an analytical GC was performed.

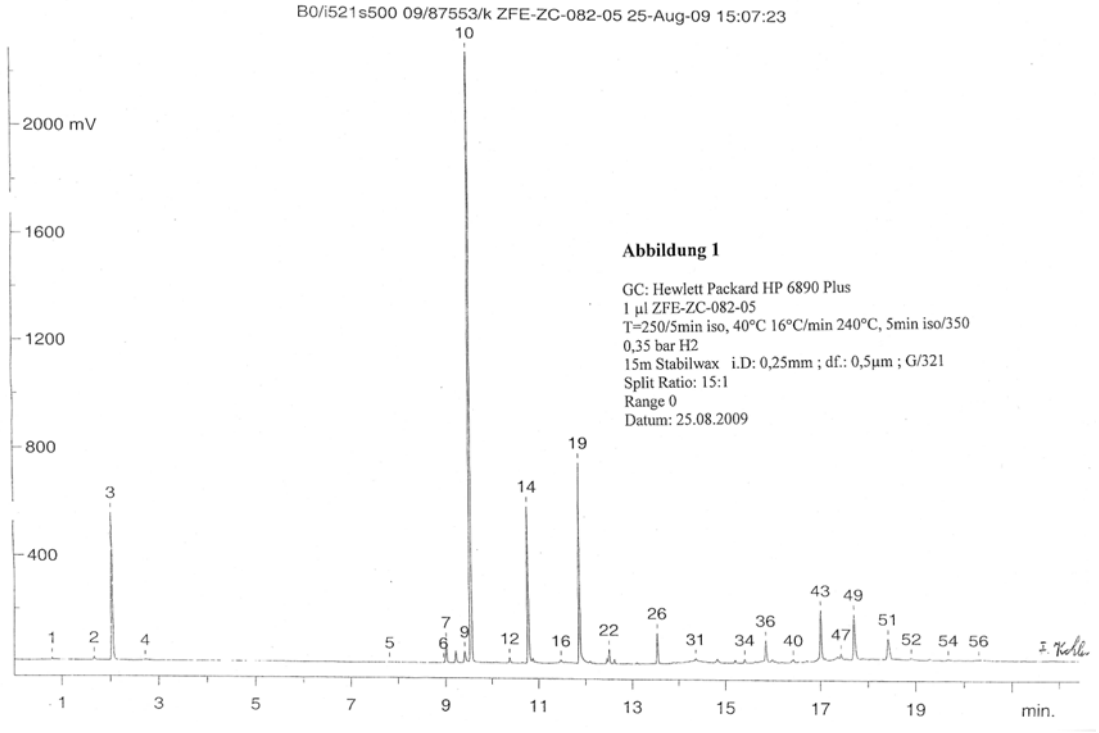

Figure S1. Analytical gas chromatogram of sample ZFE-ZC-082-05 containing **1d**. In this chromatogram peak no. 2 falls at the retention time of methanol. The chromatographic parameters are described in Figure S1.

In order to confirm methanol as the compound of peak no.2 in Figure S1, two GC-MS analyses were carried out with this sample in the selected ion monitoring (SIM) modus.

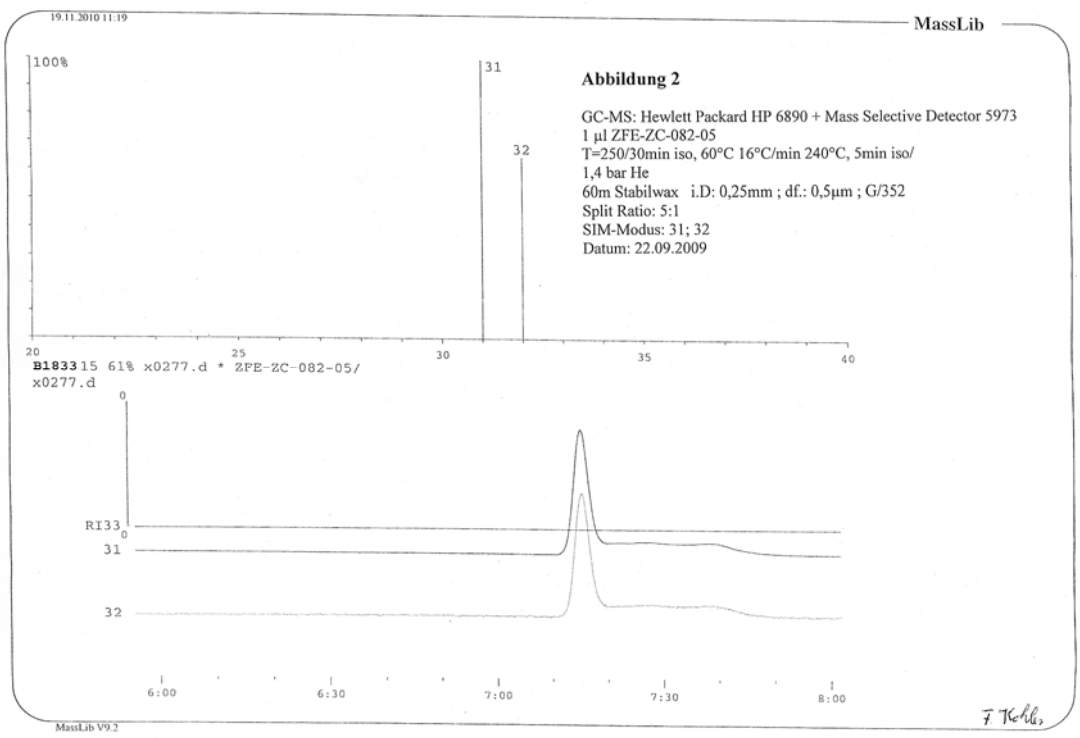

Figure S2. GC-MS analysis of sample ZFE-ZC-082-05 in the SIM modus with preselected, methanol specific masses mz 31 and mz 32. The GC separation was performed on a 60m Stabilwax capillary separating column. The chromatographic parameters are described in Figure S2.

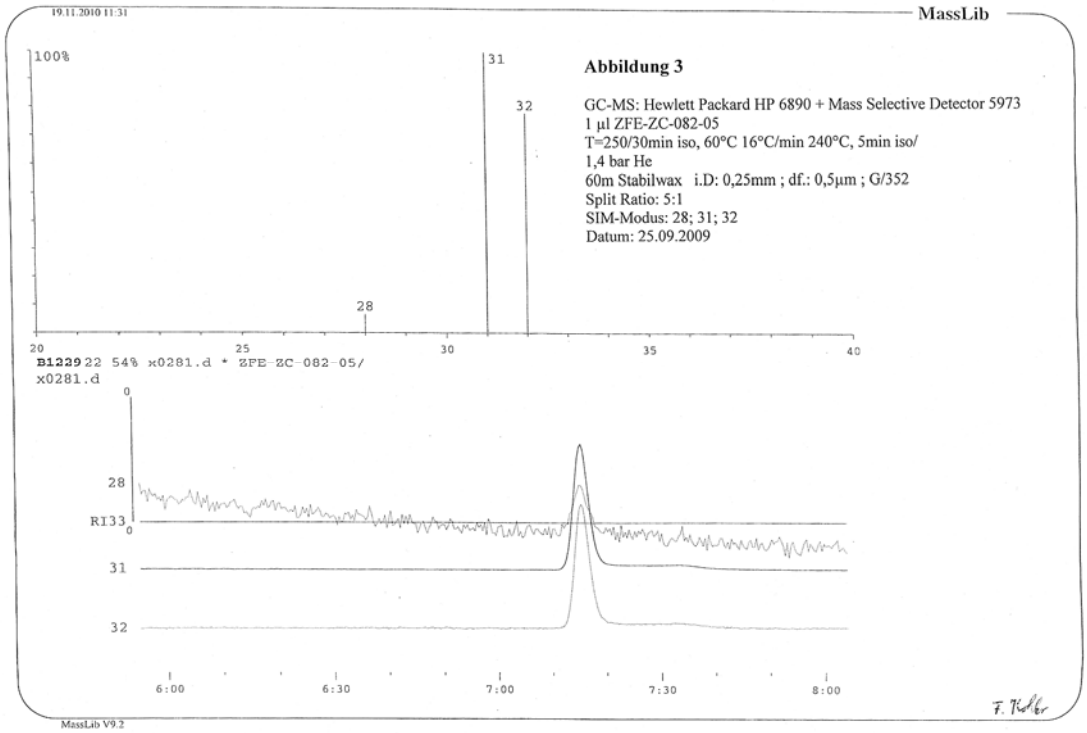

Figure S3. Additional GC-MS analysis of sample ZFE-ZC-082-05 in the SIM modus, this time additionally analyzing the N_2 specific mass mz 28, to estimate the portion of air in the sample.

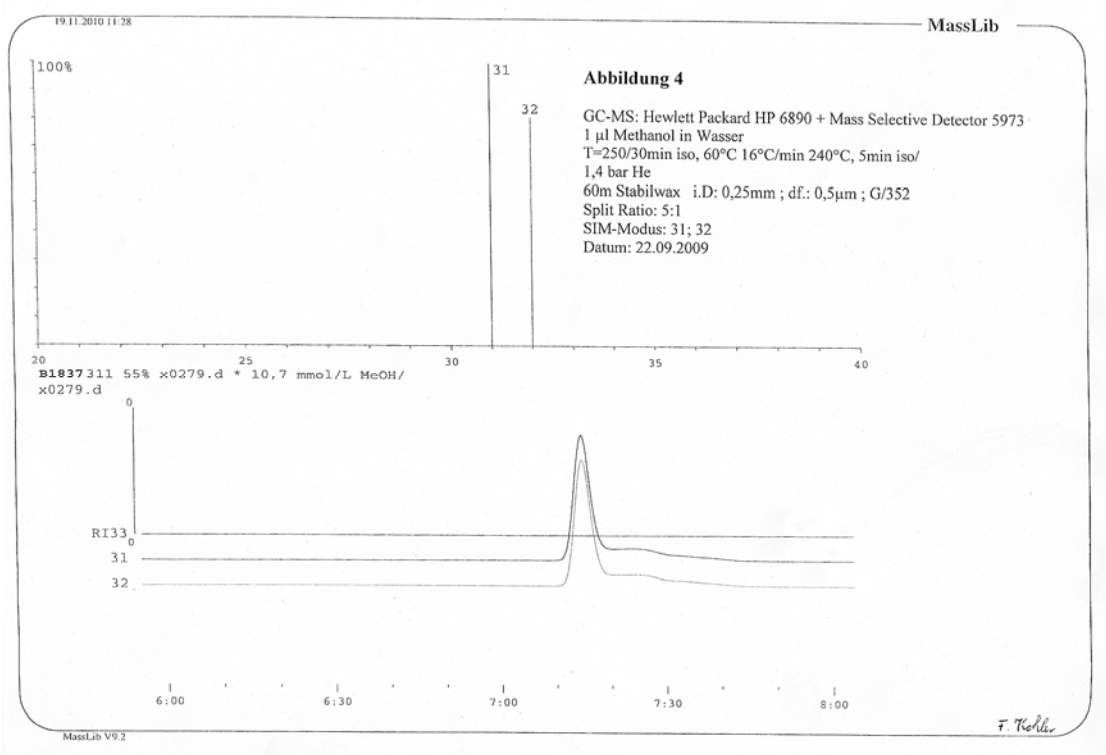

Figure S4. GC-MS analysis of a test sample containing methanol in the SIM modus (mz 31 and mz 32) to illustrate the characteristic relative ratio of the mass peaks.

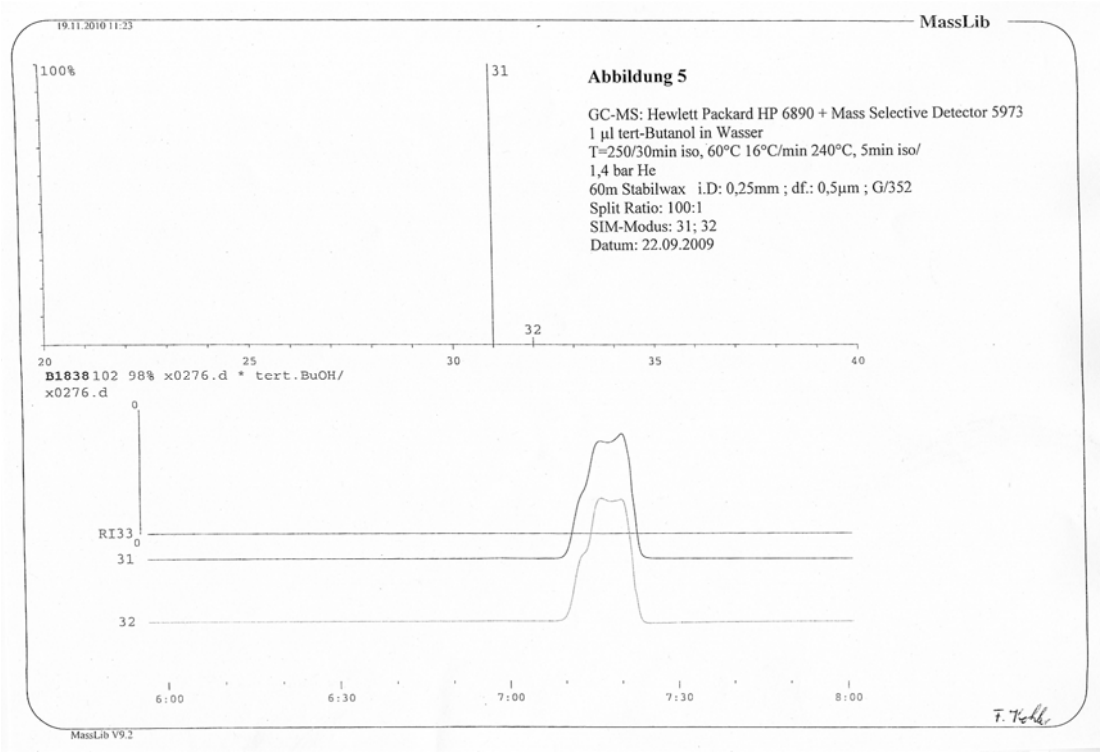

Figure S5. GC-MS analysis of a test sample containing *tert*-butanol to exclude the presence of *tert*-butanol in peak no. 2 of sample ZFE-ZC-082-05. The analysis was performed in the SIM modus using the masses mz 31 and mz 32. *Tert*-butanol shows a lower relative intensity for mz 32 than methanol (cf. Figure S4).

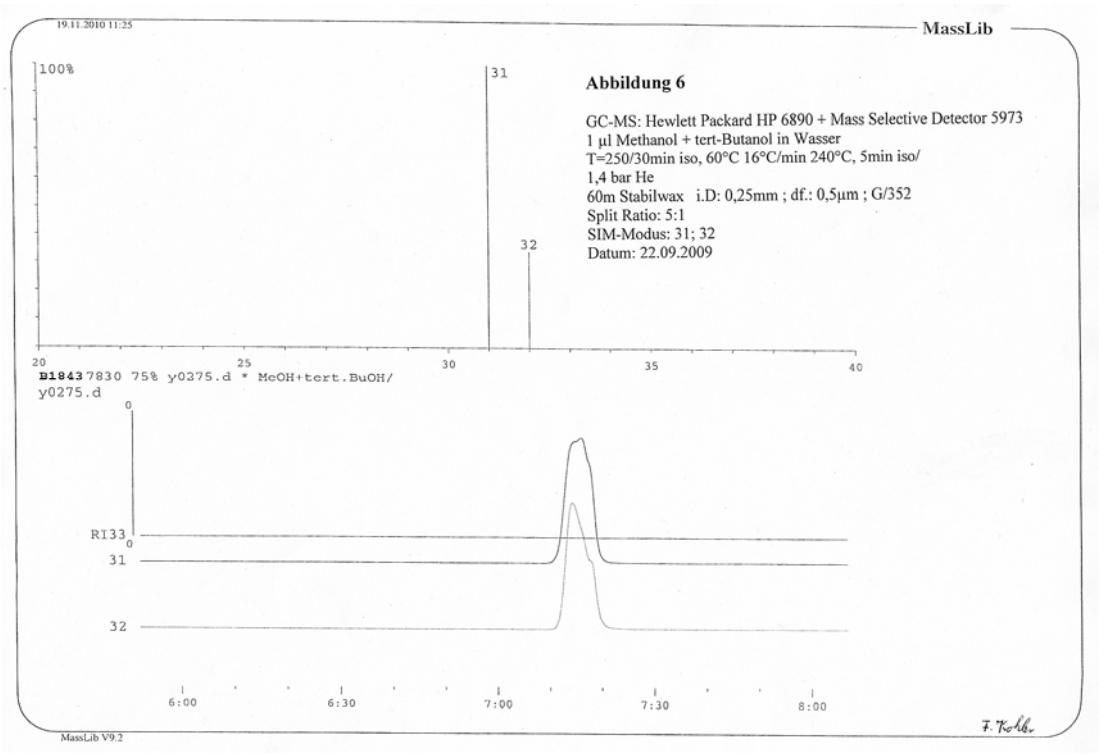

Figure S6. GC-MS analysis of a test sample containing a mixture of methanol and *tert*-butanol in the SIM-Modus focusing on the masses mz 31 and mz 32. Here, the mass mz 32 is clearly present.

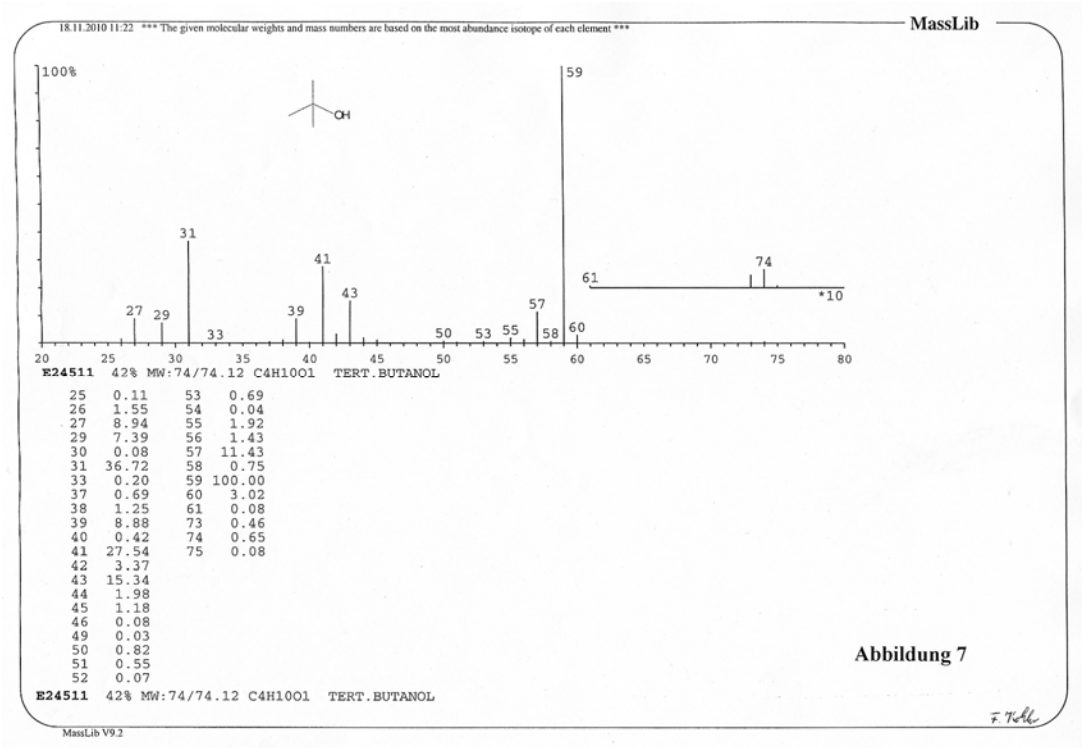

Figure S7. Additional comparative MS spectrum of *tert*-butanol obtained from the MPl-Masslib-spectra library. The mass mz 32 is absent for 1-butanol.

In parallel, the samples were analyzed using HPLC using a pulsed amperometric detection system to quantify the methanol content.

Gerät : LC-10-GPC

Operator : Hi
Sample Name :
Vial # : 24
Injection Volume : 10 uL
Data File Name : ZFE-ZC-082-05.lcd
Method File Name : Methanol.lcm

Data Acquired: 11.08.2009 17:55:54

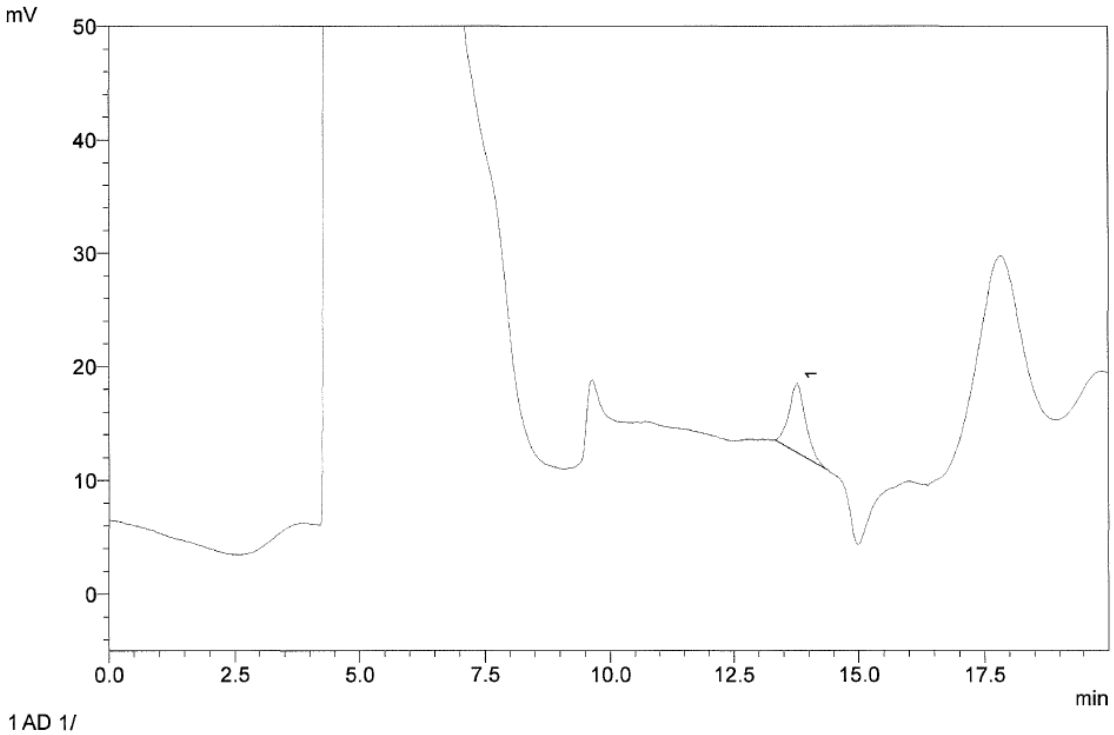

1 AD 1/

AD1 Ch1

Peak #	Ret. Time	Area %	Area	Conc.	Units	Name
1	13.77	100.00	139885	0.106	mg/mL	Methanol
Total		100.00				

Figure S8. HPLC chromatogram of sample ZFE-ZC-082-05 and methanol quantitation.

TON calculations

The TON values were calculated for the enzyme and mediator after the end of the reaction (mol product/mol enzyme).

UV-VIS spectroscopy

Prior to UV/Vis measurements[4], the protein was treated with NADPH to remove traces of compound binding to the enzyme. After this pre-treatement, the buffer was exchanged to 100 mM Tris-HCl pH 8.0, 150 mM NaCl using ultra centrifugal filters. UV/Vis spectra were recorded using UV-2401PC spectrophotometer (Shimadzu) and quartz cuvettes of 1.00 cm optical path length. All measurements were performed at 25 °C. Measured solutions contained approximately 20 µM solution of wt P450 BM3 and appropriate concentration of additives (undecanoic acid, **1e**, and *n*-octylamine). 500 mM stock solutions of additives in DMF were used. The addition of additives leads to slight precipitation, therefore the solutions were spun using top-table centrifuge and supernatant was used for the measurements.

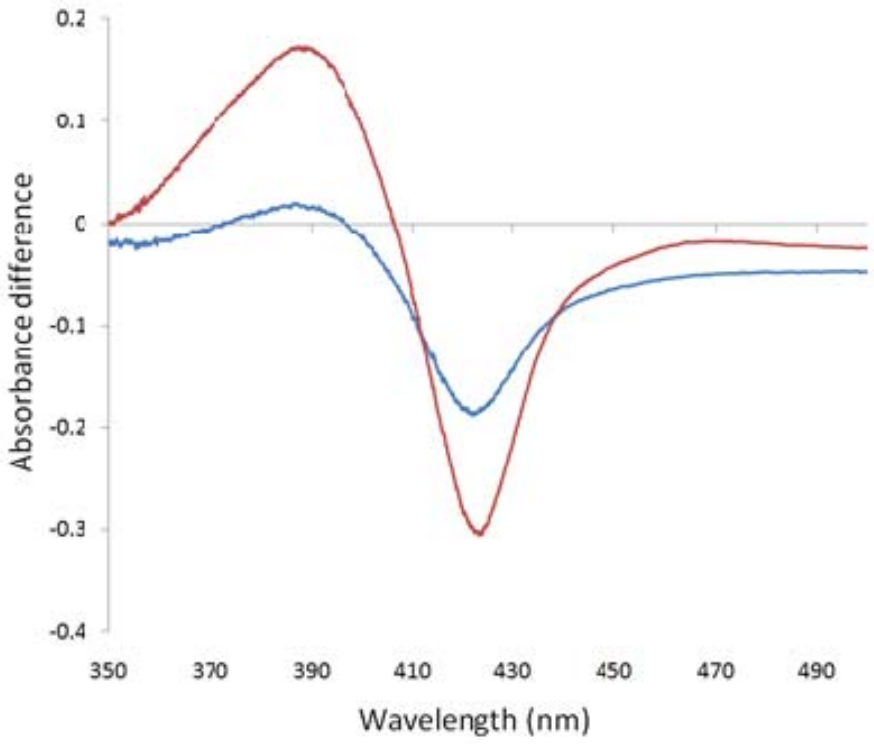

Figure S9. UV/Vis difference spectra of P450 BM3 in the presence of undecanoic acid (red) and the perfluoro-analog **1e** (blue). BM3 solution was used as a reference.

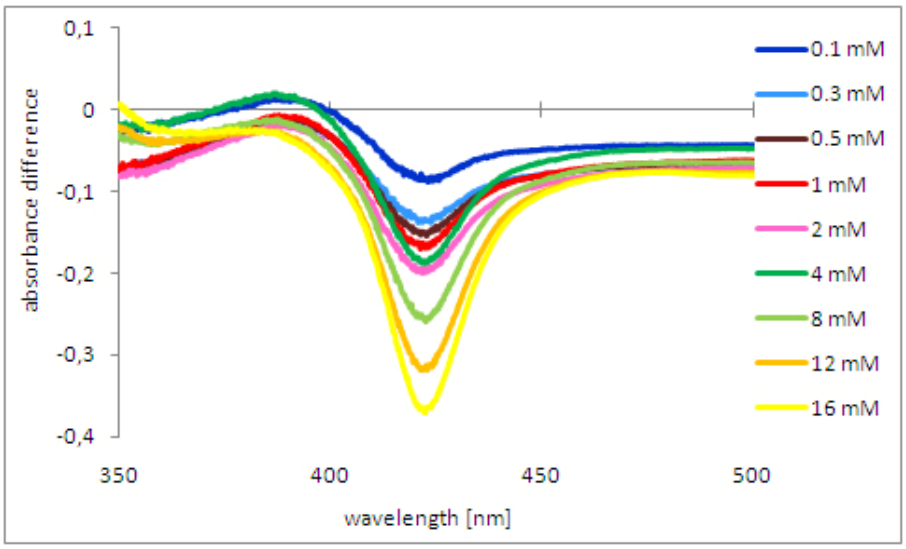

Figure S10. Difference UV/Vis spectra of P450 BM3 in presence of different concentration of **1e**. Blank cuvette: P450 BM3 mixed with the corresponding amount of DMF.

Further evidence for the binding of the perfluoro fatty acid **1e** at the active site was derived from competition experiments involving *n*-octylamine as an inhibitor. The respective guest/host interaction, characterized by coordination of the amino group to heme-Fe and hydrophobic effects between the alkyl chain and the walls of the binding pocket, has been reported to influence the UV/Vis spectra. Effectively, the appearance of the difference spectra recorded in the presence of *n*-octylamine is different from spectra observed in the presence of **1e**. The inhibitor causes a hypochromic effect in the P450 BM3 spectrum at 415 nm and a hyperchromic effect at 435 nm, in addition to a red shift of absorption maximum (Fig. S11).

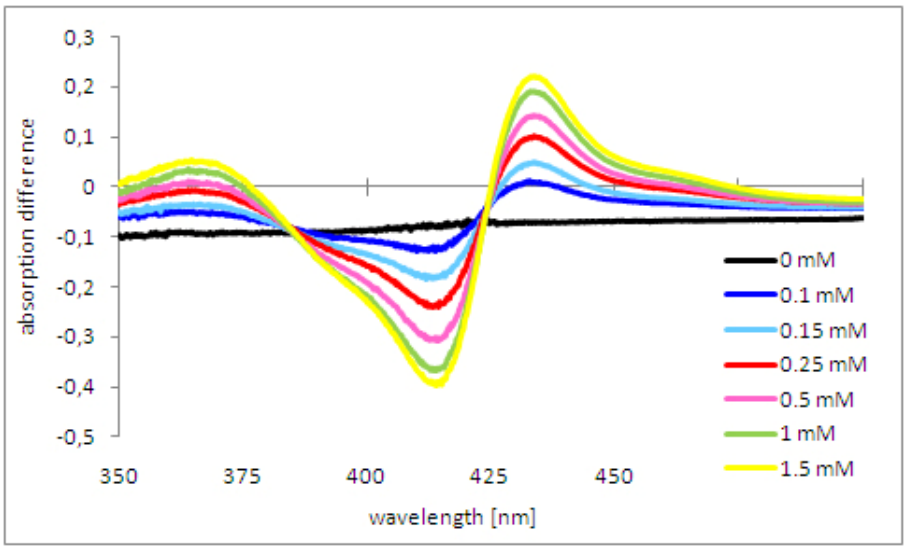

Figure S11. Difference UV/Vis spectra of P450 BM3 in presence of different concentrations of *n*-octylamine. Blank cuvette: P450 BM3 mixed with corresponding amount of DMF.

This creates the opportunity to perform competition experiments using the inhibitor *n*-octylamine and the perfluoro fatty acid **1e**. Accordingly, a mixture of P450 BM3 with *n*-octylamine was titrated using **1e**. UV/Vis difference spectra were recorded against a blank containing the enzyme and the corresponding concentration of **1e** in the absence of *n*-octylamine. The UV/Vis difference spectra are shown in Figure S12.

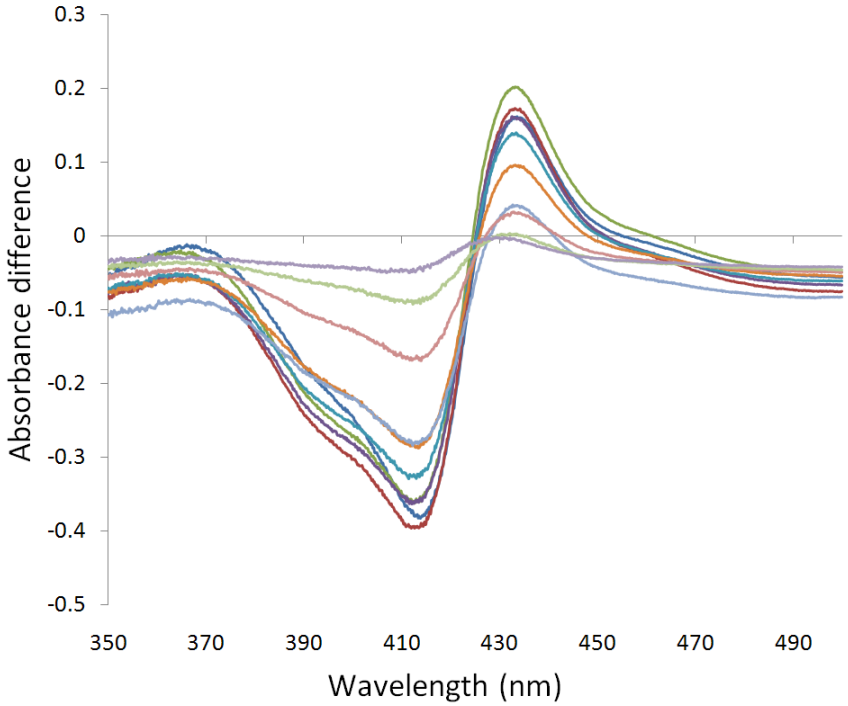

Figure S12. UV/Vis difference spectra recorded during titration experiments of P450 BM3 harboring *n*-octylamine with **1e** functioning as the titrant. BM3 solution with the corresponding concentration of **1e** was used as a reference.

A signal disappearance in the P450 BM3/*n*-octylamine UV/Vis difference spectrum with increasing **1e** concentration is clearly observed, which shows that the inhibitor is being replaced by the perfluoro fatty acid **1e**. Adding an excess of inhibitor after the titration restores the spectrum typical for the host/guest complex P450 BM3/*n*-octylamine, indicating reversible competition between the two structurally different guests.

Computational studies

In order to throw some light on the origin of the catalytic activation effect of perfluoro carboxylic acids, molecular dynamics (MD) simulations were carried out in presence and absence of the **1d**. MD

simulations were executed with the Desmond program[6] using OPLS-AA/SPC force field, and a recording interval of 1.2 ps. Long-range electrostatic interactions using Particle Mesh Ewald (PME) and van der Waals interactions were computed with a real space contributions truncated at 9 Å. Bond lengths to hydrogens were constrained by using the SHAKE algorithm. We used a RESPA integrator with time steps set to 2 fs for bonded and short-range non-bonded interactions, and 6 fs for long-range electrostatic interactions. Before every dynamic simulation, the solvated systems were relaxed into a local energy minimum using 50 steps of a hybrid method of steepest descent minimization and a limited-memory Broyden-Fletcher-Goldfarb-Shanno (L-BFGS) minimization. Additionally, the model systems were relaxed before simulation through a series of minimization and short dynamic simulations (NPT ensemble using a Berendsen thermostat and barostat) equilibrating the system at 300 K and 1 Atm. Finally, production simulations were performed for every solvated system during 5 ns, coupling the system using NPT simulation, maintaining 1 Atm at 300 K with a Martyna–Tobias–Klein barostat (relaxation time of 2 ps) and a Nose–Hoover thermostat (relaxation time of 0.5 ps). MD simulations of P450 BM3 were done using a Fe-specie in the heme cofactor which corresponds to the so called resting state.[7] In a first exploratory MD simulation of P450 BM3 in absence of any ligand and using a SPC water solvent system[8,9] with 150 mM NaCl, after 1 ns of equilibration in the productive MD simulation, recorded conformers from the following 4 ns were clustered using the Gromos algorithm[10] with a RMSD cutoff value of 0.125 Å. For substrate dockings (**1d**), the Glide program[11,12] was employed over energy minimized average structures from every cluster of conformers. Perfluorodecanoic acid (**1d**), which led to the highest activity in methane oxidation (Table 3 in the main manuscript), was successfully docked in the average minimized structure of the most populated cluster of P450 BM3 conformers.

A second round of MD simulations was run using the cluster average structure in presence and absence of the previously docked **1d** compound. Calculations were executed as described above, but this time using a mix solvent system of 1 mM methane in SPC water model pre-equilibrated at 10 bar and 300 K of temperature and then incorporated to the whole system including the P450 BM3 and perfluoro ligand. Production simulations were performed during 5 ns maintaining a pressure of 10 bar at 300 K. Recorded conformers were clustered using the Gromos algorithm and minimized average structure of each cluster calculated.

Along the simulation, **1d** adopts two principal binding modes, where its carboxy function interacts respectively with Tyr51 and Ser72 or Arg47 via hydrogen bonds, placing the activator in a positional

orientation similar to what is observed by X-ray analysis of traditional fatty acid binding. Both binding modes show the terminus of the perfluoroalkyl chain occupying a position next to the Fe-heme without causing the reorientation of the phenyl group of Phe87 with concomitant blocking of the oxyferryl porphyrin radical cation, as it has been observed in crystal structures and MD simulations for normal fatty acid with longer carbon chains. The first binding mode (binding mode I) observed in the 50 % of the MD conformers is characterized for having hydrogen bond interaction with Ser72 and interaction with Tyr51 through a water bridge. Its perfluoroalkyl chain is located closer to the Fe-heme than the second binding mode (binding mode II). In the binding mode II, represented in the 50 % of the conformers approximately, the carboxy group interacts mainly with Arg47, locating the end of the perfluoroalkyl chain in a more retracted position from the porphyrin ring (Figure S13).

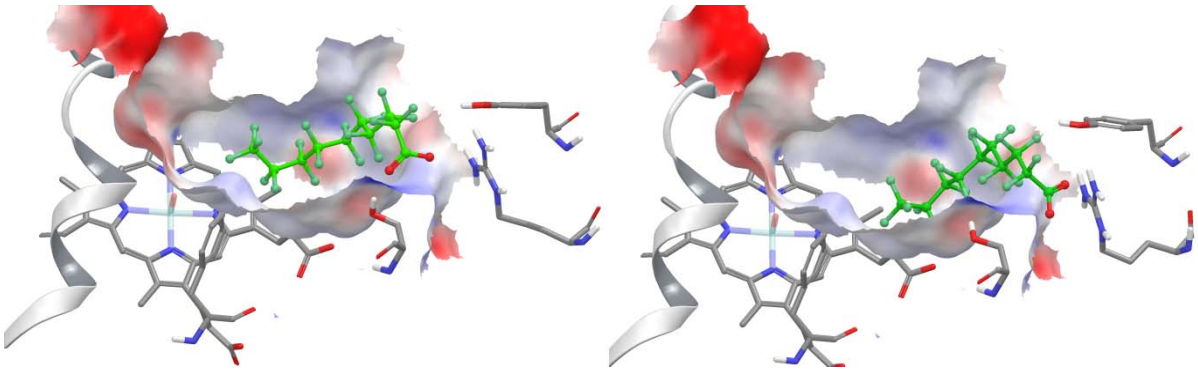

Figure S13. Binding pocket representation of P450 BM3 including compound **1d** (carbons in light green and fluorine in dark green). On the right it is represented the first main binding mode in which the ligand carboxy group interacts with Ser72 and Tyr51. On the left it is shown the second binding mode having the carboxy function interacting with Arg47. Binding pocket surface is colored according with its electrostatic potential (red: positive, blue: negative, white: neutral). Helix I is given as a landmark.

Subsequently, docking analysis of methane were performed using the minimized average structure of the three main cluster obtained from the MD calculations in presence and absence of **1d**. At this point a decision had to be made as to which Fe-species should be employed in next docking analyses following the second round of MD simulations. In view of the known hydroxylation mechanism based on biophysical and theoretical studies,[7] we decided to use the neutral form of the positively charged activated oxygen intermediate proposed in the literature (also called Cpd I), which is believed to participate in rate- and regioselectivity-determining hydrogen abstraction as the initial part of oxidative C-H activation. The

advantage of using neutral Cpd I as a hypothetical species is the fact that the respective force fields are available,[13] while also reflecting the real steric situation. In the case of docking calculations in presence of **1d**, P450 BM3 and the different binding modes of fluorinated substrate were included for the receptor grid constructions using the Glide program. The results showed that good binding poses for methane were only obtained for the binding mode I of **1d**, in which the methane occupies a positions near the catalytically active Fe-heme within a distance and angle from the active oxygen in accordance with the geometric values for hydrogen abstraction in P450s[7,14] (see Figure S13 and Figure 1 in the main manuscript). Methane cluster of binding poses come to lie between a hydrophobic region in the wall of the active site and the perfluoroalkyl extreme of the activator (compound **1d**). In the case of the binding mode II, the pulling effect due to the Arg47-carboxyl interaction thereby influencing the perfluorodecanoic acid position, generates a larger space in the active site where methane can be more evenly distributed without energetically favored binding poses. Docking calculations in absence of the perfluorinated ligand did not show any binding poses as well.

References

1. J. Sanchis, L. Fernandez, J. D. Carballeira, J. Drone, Y. Gumulya, H. Hobenreich, D. Kahakeaw, S. Kille, R. Lohmer, J. J. P. Peyralans, J. Podtetenieff, S. Prasad, P. Soni, A. Taglieber, S. Wu, F. E. Zilly, M. T. Reetz, *Appl. Microbiol. Biotechnol.* **2008**, *81*, 387–397.
2. U. Schwaneberg, A. Sprauer, C. Schmidt-Dannert, R. D. Schmidt, *J. Chromatogr. A* **1999**, *848*, 149–159.
3. T. Omura, R. Sato, *J. Biol. Chem.* **1964**, *239*, 2370–2378.
4. Y. Yoshida, H. Kumaoka, *J. Biochem.* **1975**, *78*, 455–468.
5. W. R. LaCourse, D. C. Johnson, M. A. Rey, R. W. Slingsby, *Anal. Chem.* **1991**, *63*, 134-139.
6. (a) K. J. Bowers, E. Chow, H. Xu, R. O. Dror, M. P. Eastwood, B. A. Gregersen, J. L. Klepeis, I. Kolossváry, M. A. Moraes, F. D. Sacerdoti, J. K. Salmon, Y. Shan, D. E. Shaw, *Proceedings of the ACM/IEEE Conference on Supercomputing (SC06)*, Tampa, Florida, **2006** November**,** 11–17. (b) D. S. Cerutti, R. Duke, P. L. Freddolino, H. Fan, T. P. Lybrand, *J. Chem. Theory Comput.* **2008**, *4*, 1669-1680. (c) I. T. Arkin, H. Xu, M. Ø. Jensen, E. Arbely, E. R. Bennett, K. J. Bowers, E. Chow, R.

O. Dror, M. P. Eastwood, R. Flitman-Tene, B. A. Gregersen, J. L. Klepeis, I. Kolossváry, Y. Shan, D. E. Shaw, *Science (Washington, DC, U. S. A.)* **2007**, *317*, 799–803.

7. S. Shaik, S. Cohen, Y. Wang, H. Chen, D. Kumar, W. Thiel, *Chem. Rev.* **2010**, *110*, 949–1017.
8. H. J. C. Berendsen, J. P. M. Postma, W. F. van Gunsteren, J. Hermans, Intermolecular Forces, **1981**, Ed. Pullmann B. (Reidel, Dordrecht), p. 331.
9. C. D. Berweger, W. F. van Gunsteren, F. Müller-Plathe, *Chem. Phys. Lett.* **1995**, *232*, 429–436.
10. X. Daura, K. Gademann, B. Jaun, W. F. van Gunsteren, A. Mark, *Angew. Chem. Int. Ed.* **1999**, *38*, 236–240.
11. (a) R. A. Friesner, J. L. Banks, R.B. Murphy, T. A. Halgren, J. J. Klicic, D. T. Mainz, M. P. Repasky, E. H. Knoll, M. Shelley, J. K. Perry, D. E. Shaw, P. Francis, P. S. Shenkin, *J. Med. Chem.* **2004**, *47*, 1739–1749. (b) T. A. Halgren, R. B. Murphy, R. A. Friesner, H. S. Beard, L. L. Frye, W. T. Pollard, J. L. Banks, *J. Med. Chem.* **2004**, *47*, 1750–1759.
12. Schrödinger, LLC Maestro 8.5 User Manual (Schrödinger Press, New York, 2008).
13. A. Seifert, S. Tatzel, R. D. Schmid, J. Pleiss, *Proteins* **2006**, *64*, 147–155.
14. Y. Zhang, P. Morisetti, K. Jeffery, L. Smith, L. Hai, *Theor. Chem. Account* **2008**, *121*, 313–319.